2023

Under Ice Photosynthetic Primary Production and Dark Carbon Fixation in a Temperate Freshwater System

Vanessa Cubillos Tellez
Michigan Technological University, vcubillo@mtu.edu

UNDER ICE PHOTOTSYNTHETIC PRIMARY PRODUCTION AND DARK CARBON FIXATION IN A TEMPERATE FRESHWATER SYSTEM

By

Vanessa Cubillos Tellez

A THESIS

Submitted in partial fulfillment of the requirements for the degree of

MASTER OF SCIENCE

In Biological Sciences

MICHIGAN TECHNOLOGICAL UNIVERSITY

2023

This thesis has been approved in partial fulfillment of the requirements for the Degree of MASTER OF SCIENCE in Biological Sciences.

Department of Biological Sciences

Thesis Advisor:	*Dr. Trista J. Vick-Majors*
Committee Member:	*Dr. Amy M. Marcarelli*
Committee Member:	*Dr. Michael R. Gretz*
Department Chair:	*Dr. Chandrashekhar P. Joshi*

Table of Contents

Acknowledgements

I am incredibly grateful for my advisor, Dr. Trista J. Vick-Majors, who provided me with this research opportunity and served as a wonderful mentor throughout this process. Without her expertise, encouragement, and guidance, this research would not have been possible. I would also like to thank Dr. Amy M. Marcarelli, Dr. Michael R. Gretz for serving on my committee and providing thoughtful feedback and support on my project.

Thank you to all of the students who helped in the lab and field, especially to Alex Baker and Aleksander Milosevic who helped with the radioisotope experiments. A huge thank you to Maci Quintanilla for her assistance and support on this project. I would also like to thank my friends and family for their constant support and belief in me.

My research was funded by the Michigan Chapter North American Lake Management Society (McNALMS) and the Michigan Lakes and Streams Association (MLSA), funding from the College of Arts and Sciences at Michigan Technological University, and startup funds from Michigan Technological University and the Michigan Space Grant Consortium award (#SUBK00015391) to TJV-M.

List of Abbreviations

PPR – Primary Production Rates

PPP – Photosynthetic Primary Production

DCF – Dark Carbon Fixation

PAR – Photosynthetically Active Radiation

DOC – Dissolved Organic Carbon

POC – Particulate Organic Carbon

TDN – Total Dissolved Nitrogen

SRP – Soluble Reactive Phosphorus

DO – Dissolved Oxygen

GLM – Generalized Linear Model

Abstract

Ice-covered lakes are vulnerable to environmental change, especially those in the Northern Hemisphere where ice cover is rapidly declining due to global warming. These changes can alter metabolic processes and disrupt carbon cycling driven by primary producers who form the base of the food chain and are key to sustaining ecosystem function. Photosynthetic primary production and dark carbon fixation under the ice in the Keweenaw Waterway, a temperate freshwater system that is ice-covered for ~3 months out of the year, were studied using a carbon isotopic labeling (^{14}C-bicarbonate) technique. Water samples were collected weekly during ice-cover and monthly during summer from winter 2021 into 2022. Environmental conditions were also measured at the time of sampling. Results revealed photosynthetic primary production was substantially reduced during ice cover, however, there was a relatively high abundance of chlorophyll-a present during the ice-covered periods suggesting photoadaptation. Dark carbon fixation was also suppressed during the ice covered period compared to the open water period. Extracellular release of dissolved organic carbon was substantially higher in dark carbon fixation compared to photosynthetic primary production suggesting dark carbon fixation may be an important source of dissolved organic carbon. Together, these findings give insight into the relative importance of photosynthetic primary production and dark carbon fixation to aquatic carbon production and its response to changing environmental conditions.

1 Introduction

Earth's surface contains an estimated 117 million lakes, more than half of which are subject to seasonal freezing (Block et al. 2019). The ice-covered season is now recognized as a time of continuing biological activity, which is important for the year-round ecosystem function (e.g., carbon flow; Gerten and Adrian 2000). Many seasonally ice covered lakes are at risk for losing their ice cover as atmospheric temperatures rise (Sharma et al. 2019), but despite their importance and the risk of ice loss, the biological processes under ice in temperate freshwaters remain to be fully understood. Here, I examine the activity of microorganisms responsible for carbon fixation (primary production) under ice in a temperate freshwater system.

1.1 Primary Producers in Aquatic Systems

1.1.1 Photosynthetic Primary Producers

Primary production is a major source of new carbon to aquatic systems and is carried out by photosynthetic primary producers (photoautotrophs) and chemoautotrophs. Photoautotrophs rely on incoming photosynthetically active radiation (PAR) as an energy source for essential processes including the transformation of inorganic carbon to organic carbon. These organisms include members of the Eukaryota and the Bacteria (eukaryotic phytoplankton and Cyanobacteria). Two major groups of eukaryotic phytoplankton include diatoms and dinoflagellates. Diatoms are unicellular phytoplankton that have unique cell walls made of silica. They make up a major group in freshwater spring phytoplankton blooms. Dinoflagellates are unicellular and, unlike diatoms, have flagella allowing them to be mobile.

Cyanobacteria make up a major part of the photosynthetic phytoplankton community (Callieri 2008). They can contribute an important proportion of total primary production in the ocean as well as freshwater ecosystems (Ivanikova et al. 2007). Anoxygenic phototrophic bacteria can also contribute to primary production where oxygen is absent, although their overall contribution is small compared to oxygenic phototrophs (Kirchman 2018). Additional metabolic strategies exist, such as aerobic anoxygenic phototrophy, which can be conducted by bacteria that use light as an energy source but use organic

matter as a carbon source (photoheterotrophs; Table 1). Together, these photosynthetic organisms form the foundation of aquatic food webs through their production of organic carbon.

Table 1: Metabolic strategies among microbial groups

	Photoautotrophy	**Chemoautotrophy**	**Heterotrophy**	**Mixotrophy**
Energy Source	Sunlight (photo-)	Chemical (chemo-)	Organic matter (-heterotroph)	Use multiple metabolic strategies
Carbon Source	CO_2 (-autotroph)	CO_2 (-autotroph)		

1.1.2 Chemoautotrophic Bacteria and Archaea

In systems where light is limited and/or energy is available from the catalysis of chemical reactions, primary production carried out by chemoautotrophic bacteria and archaea that do not require light to power their metabolisms (hereafter, "dark carbon fixation") plays an important role (Cavaliere and Baulch 2018, Vick-Majors and Priscu 2019). These organisms oxidize or reduce inorganic compounds to conserve energy, rather than using light as their energy source. Examples of inorganic compounds that may serve as energy sources for chemoautotrophs include molecular hydrogen, hydrogen sulfide, ferrous iron, and ammonium. Their ability to use a range of inorganic compounds allows chemoautotrophy to be widely distributed metabolic strategy across environments. Sulfur-oxidizing and iron-oxidizing chemoautotrophs are commonly found in acidic environments, whereas ammonia-oxidizing chemoautotrophs are widespread in freshwater environments (Auguet et al. 2011). Furthermore, chemoautotrophy can occur with or without oxygen present, expanding their capabilities of transforming carbon in the environment, although more energy is conserved in the presence of oxygen.

Ammonia-oxidizing bacteria, ammonia-oxidizing archaea, and nitrite-oxidizing bacteria carry out nitrification, which is the oxidization of ammonium and nitrite to nitrate. Studies have shown nitrification to be an important process during ice cover, in some cases leading to the accumulation of nitrate over winter (Massé et al. 2019,

Knowles and Lean 1987, Powers et al. 2017). Ammonia-oxidizing archaea may play a larger role in ammonia oxidation compared to bacteria (Tolar et al. 2016), especially in freshwater systems when ammonium concentrations are low (Massé et al., 2019). Ammonia-oxidizing archaea are adapted to lower substrate concentrations (Jung et al. 2022, Martens-Habbena et al. 2009) allowing them to potentially dominate oligotrophic lakes (Könneke et al. 2005) such as Lake Superior (Small et al. 2013). The relative importance of their overall contribution to carbon fixation remains unknown in most freshwater systems.

1.2 Primary Production Under Ice

1.2.1 Factors Influencing Primary Production

1.2.1.1 Water Temperature

Temperature is one of the most important drivers of ice formation (Livingstone and Adrian 2009). With rising temperatures, the onset of ice cover can be delayed, which can influence metabolic rates of microorganisms as high temperatures can lead to high rates of microbial activity (Hoppe et al. 2008, Huang et al. 2021). Not only can water temperature influence microbial activity, but it can also be important in determining the abundance and composition of primary producers. Studies have shown differences in community structure between the ice covered and open water period (Özkundakci et al. 2016). One reason for this may be because primary producers have different optimal water temperatures. Primary producers that are tolerant of cold temperatures can outcompete other primary producers allowing them to prevail under ice (Vincent and Vincent 1982). Most freshwater phytoplankton are adapted to temperatures between 10-30°C (Butterwick et al. 2005). Some cyanobacteria favor higher temperatures compared to other phytoplankton like diatoms and green algae (Reynolds 2006). Optimal temperatures for diatoms are between 5-25°C (Butterwick et al. 2005), while optimal temperatures for some cyanobacteria are between 25-30°C (Jöhnk et al. 2008). These temperature ranges, however, are based on laboratory studies or samples collected during the summer period. Less attention has been given to the potential adaptations of phytoplankton to low temperatures during winter.

1.2.1.2 Nutrients

Nutrients such as phosphate and nitrate make up cell components that are critical for microbial growth, and their availability often limits primary production in aquatic systems. Phosphorus is a primary limiting nutrient in temperate freshwater ecosystems. Nitrogen is often seen as the second limiting nutrient behind phosphorus (Sterner 2008); however, this is not the case for Lakes Superior. Nitrogen species such as nitrate have increased over the years in Lake Superior (Baehr and McManus 2003). Winter is typically viewed as a critical period for nutrient regeneration. Nutrients are expected to be depleted during summer when conditions are favorable for primary producers (e.g., warm water temperatures, abundant light), whereas during the ice covered period, there is a less demand for nutrients by primary producers. This allows nutrients to be regenerated by heterotrophic microorganisms under the ice.

1.2.1.3 Photosynthetically Active Radiation

Photosynthetically active radiation (PAR) in the range of 400 nm to 700 nm can be a limiting factor for primary producers that require light as an energy source. Ice cover limits the penetration of PAR (Arst et al. 2006, Tanabe et al. 2008). The amount of PAR transmission through ice depends on snow cover (Jewson et al., 2009) and on the quality of the ice itself, with black ice (clear ice) transmitting more PAR than white ice (Weyhenmeyer et al., 2022). Up to 95% PAR transmission has been observed in some studies when the ice is snow-free (Bolsenga 1981) and as little as 2% PAR transmission when snow is present; both light levels still allow photosynthetic primary production to take place (Cota 1985, Garcia 2019). Permanently ice-covered Antarctic lakes sustain phytoplankton populations that are adapted to perennially low light levels (Morgan-KM et al. 2016). Despite low levels of light, lakes can still experience high rates of photosynthetic primary production that produce phytoplankton blooms during winter (Dokulil and Herzig 2009). Lake Erie experienced a large phytoplankton bloom, with chlorophyll-a concentrations of over 70 µg L^{-1}, which was dominated by the diatom *Aulacoseira islandica* within the ice or directly below the ice (Twiss et al. 2012). Photosynthetic primary production has also been observed to increase during snow melt as light penetration increases (Kelley 1997, Salonen et al. 2009). These light conditions

under ice play a crucial role in the activity, abundance, and composition of photosynthetic primary producers.

1.2.1.4 Primary Production During the Open Water Period

Warm temperatures, nutrient input, and high levels of PAR during the open water period are favorable to primary producers leading to high rates of PPR. Understanding the aquatic carbon production during the open water period is important. However, this is only looking at a portion of what happens throughout the year. It has been shown winter dynamics can play an influential role in the productivity of the whole lake system (Hampton et al. 2017). For example, early ice break-up can cause an early start to stratification, which is closely tied to spring phytoplankton blooms (Winder and Schindler 2004). Early events of phytoplankton blooms can influence the following season potentially shifting trophic interactions during the open water period (Winder and Schindler 2004). Thus, looking at the ecosystem across seasons can provide better insight into microbial processes and how they may respond to changes in the environment especially as ice cover is expected to continue to decline (Kirillin et al. 2012, Lemke et al. 2007).

1.3 Importance of Primary Producers

Photoautotrophs and chemoautotrophs are crucial to aquatic ecosystem function due to their major contributions to biogeochemical cycles that sustain higher trophic levels in the ecosystem (Newton et al. 2011). Because photoautotrophs and chemoautotrophs differ in how they capture energy, they may respond differently to the changing environmental conditions discussed above, which can alter the amount of newly synthesized carbon going into the system. This can have implications for higher trophic levels in the system that require fixed carbon to power their metabolisms. Therefore, understanding the activities and responses of photoautotrophs and chemoautotrophs to ice cover is critical. Photoautotrophic production rates are low during ice cover, relative to ice-free periods (Figure 1). This decrease in photoautotrophic productivity during ice cover can also be associated with differences in the amount of fixed carbon utilized for biomass production (referred to in this thesis as the particulate fraction) or released into

the environment as dissolved organic carbon (referred to in this thesis as the dissolved fraction; Sharp 1993). On the other hand, dark carbon fixation by chemoautotrophs may contribute a considerable amount of newly-fixed organic carbon during ice cover, because they do not rely on light as an energy source (Figure 1).

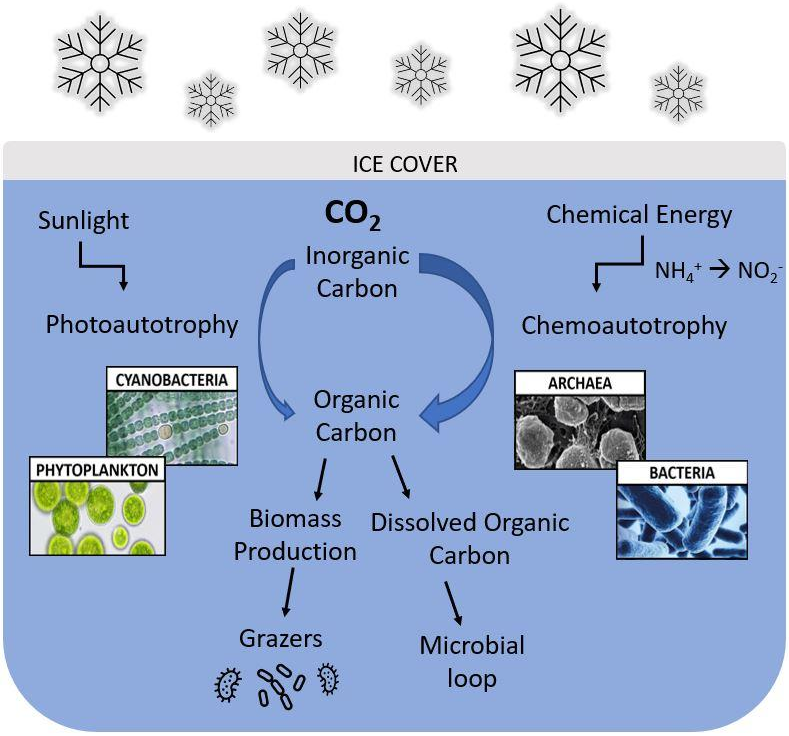

Figure 1: Photosynthetic primary production and dark carbon fixation during ice cover. The size of the arrows shows the relative expected contributions to inorganic carbon fixation from photoautotrophs and chemoautotrophs. Nitrification is shown as a potential energy generating pathway to fuel chemolithoautotrophy (referred to herein as chemoautotrophy). Photoautotrophy may be conducted by eukaryotic phytoplankton or cyanobacteria; chemoautotrophy is conducted by bacteria and/or archaea. The newly fixed carbon can be used by grazers. Dissolved organic carbon is cycled through heterotrophic bacteria and/or archaea, forming the microbial loop.

1.4 Objectives and Hypotheses

The objective of this study was to address the dynamics of photosynthetic primary production and dark carbon fixation under ice and to determine the relative importance of

these processes to aquatic carbon production. To address this, experiments were conducted to, (1) measure rates of photosynthetic primary production and dark carbon fixation, (2) determine whether prokaryotic or non-prokaryotic groups are primary contributors to wintertime carbon fixation, (3) determine how much fixed carbon is partitioned into the dissolved fraction compared to the particulate fraction.

I hypothesized that (i) due to unfavorable winter conditions including limited light penetration (Jewson et al. 2009), cold temperatures (Özkundakci et al. 2016), and ice/snow coverage (Garcia et al. 2019), photosynthetic primary production will be reduced relative to dark carbon fixation under ice, making chemoautotrophy an important metabolic process and, (ii) primary production will be preferentially partitioned into the particulate fraction relative to the dissolved fraction as resources are limited under the ice. To test these hypotheses, I experimentally measured rates of photosynthetic primary production and dark carbon fixation using a carbon isotopic labeling (^{14}C-bicarbonate) technique weekly during the ice covered periods in 2021 and 2022, and at biweekly or monthly frequencies at other times of year.

2 Methods

2.1 Study Site

The Keweenaw Waterway is a mesotrophic, temperate, freshwater system that is ice-covered for ~3 months out of the year located in the Upper Peninsula of Michigan (~47.12° N – 88.54° W). It is partly natural and partly artificial and is a transportation corridor and an important recreational site for residents and visitors. The waterway is approximately 38 km in length (Churchill et al. 2004) and has an average depth of 7.6 m (~5 m at the sample collection site) that runs through Portage Lake and connects to Lake Superior at the North and South Entries of the Keweenaw Peninsula (Figure 2). With access to both water sources and wind-driven currents, the Keweenaw Waterway can be dynamic, however, during the ice-covered period, the waterway experiences limited water movement and horizontal mixing (Churchill et al. 2004). Butler et al. (2019) also observed long-term stability of microbial communities under-ice, suggesting conditions under ice may be more stable compared to the ice-free period.

Figure 2: Map of the Keweenaw Waterway in the Upper Peninsula of Michigan. Image provided by Google Earth.

2.2 Sample Collection

A sampling hole was made adjacent to a dock at the Great Lakes Research Center at Michigan Technological University using an ice spud, followed by the use of a strainer to scoop up any floating ice chunks at the surface of the hole. Use of the dock as a sampling platform allowed for access across seasonally-variable weather conditions. Sample collection occurred weekly during ice-cover in 2021 (samples were incubated *in situ* during this period) and 2022 (samples were placed in a lighted incubator chamber [Percival Scientific, Model AL-30L2] during this period; details below), biweekly during the transitional periods, and monthly during periods of no ice-cover. Water samples were collected 30 minutes after sunrise from 1 m below the water surface into acid washed and ultrapure water rinsed HDPE amber bottles using a peristaltic pump (Geotech). Samples were used to determine primary production as light and dark incorporation of ^{14}C-bicarbonate, alkalinity, macronutrient concentrations (soluble reactive phosphorus [SRP] and total dissolved nitrogen [TDN]), and dissolved organic carbon (DOC). Samples for the determination of chlorophyll-a were collected into ultrapure water rinsed HDPE amber bottles. Water samples were immediately brought into the lab for processing and then stored frozen at -20 ^{o}C (macronutrients) or at 4 ^{o}C (DOC) until further analysis.

2.3 Physical and Chemical Parameters

Physical (ice thickness, snow coverage, temperature, and underwater photosynthetically active radiation [PAR]) and chemical soluble reactive phosphorus (SRP), total dissolved nitrogen (TDN), dissolved organic carbon (DOC), dissolved oxygen (DO), conductivity, pH, and alkalinity) parameters were measured *in situ* at time of sample collection or on processed and stored samples. Ice thickness and snow coverage were recorded using a measuring tape (cm). Temperature, pH, conductivity, and dissolved oxygen were determined using an AquaTROLL 500 multiparameter sonde (In-Situ, U.S.) at 1 m depth below the surface. Underwater PAR was determined immediately below the water surface and at 1 m were measured with a LI-COR LI-193 Spherical Underwater Quantum Sensor (LI-COR Biosciences, U.S.). For lab-based incubations, PAR was measured at solar noon the day before sample collection immediately below the water surface and at 1 m depth to approximate the maximum PAR for sample exposure.

PAR in the incubator was logged with a microCache and full-spectrum quantum PAR sensor (Apogee Instruments) during lab-based incubations. Samples for SRP were filtered through combusted (450°C for 4 hours) 25 mm GF/F filters into acid washed (10% HCl) 125 ml HDPE bottles and stored at -20°C until analysis. Samples for DOC and TDN were filtered through combusted (450°C for 4 hours) 25 mm GF/F filters into acid washed (10% HCl) and combusted (450°C for 4 hours) 50 ml amber vials capped with PTFE lined caps and stored at 4°C until analysis. Two replicates of SRP and TDN were analyzed using a SEAL Analytical AQ2 Discrete autoanalyzer. Two replicates of DOC were analyzed using a Shimadzu TOC-L_{CPH} analyzer. All three analytes (SRP, TDN, and DOC) were measured in the AQUA lab at Michigan Technological University. Total alkalinity (mg L^{-1}) was measured using a digital titrator test kit (Hach, Model AL-DT) in a 250 mL flask containing 25 mL of sample water and diluted to 100 mL with deionized water. Phenolphthalein powder was added followed by Bromcresol Green-Methyl Red powder, allowing each to dissolve completely and the solution was titrated with sulfuric acid (0.1600 N). Dissolved inorganic carbon (mg L^{-1}) was calculated using total alkalinity, *in situ* pH and water temperature, and the conversion factors in Wetzel and Likens (2000).

2.4 Biological Parameters

2.4.1 Chlorophyll-a

Samples for chlorophyll-a were determined fluorometrically using a previously described method (Welschmeyer 1994). Briefly, 500 ml of sample water was passed through a 25 mm GF/F filter. Filters were placed into a glassine envelope and stored in a dark freezer (-20 ^{o}C) until extraction in 90% acetone and analysis using a calibrated Trilogy Laboratory Fluorometer (Turner). A serial dilution in 90% acetone was made using a 1 mg chlorophyll-a standard from *Anacystis nidulans* algae (Sigma-Aldrich) to produce the standard curve on the fluorometer (0.110, 0.460, and 4.580 mg L^{-1}).

2.4.2 Net Photosynthetic Primary Productivity and Dark Carbon Fixation

Incubations for net photosynthetic primary production and dark carbon fixation were conducted in triplicate using the ^{14}C method (Steemann Nielsen 1952). ^{14}C-bicarbonate (0.1 μCi ml^{-1} final concentration) was added to clear acid washed (10% HCl) polycarbonate bottles containing 30 ml of sample water. Samples were incubated *in situ* by clipping mesh (light treatments) or opaque (dark treatments) bags containing incubation bottles to an apparatus on the side of the dock and suspending the bottles at the depth they were collected from (2021) or placed in a lighted incubator (Percival; 2022) for ~12 hours. During ice cover in 2022, incubations were set as close to *in situ* light and temperature as possible. The lowest achievable light and temperature settings on the incubator were ~ 40 μmol photons m^{-2} s^{-1} and 1°C, respectively. Each experiment consisted of five treatments conducted in triplicate: light (photosynthetic primary production; as close to *in situ* light as possible), light + chloramphenicol (10 μg ml^{-1} final concentration; an antibiotic inhibitor of prokaryotes), dark (dark carbon fixation), dark + chloramphenicol, and a killed control. Killed controls were produced by either amending with 100% Trichloroacetic acid (5% final concentration; Vick-Majors and Priscu 2019) (January 2021 to 22 October 2021), or filtration through a 0.2 μm filter (November 2021 to 26 August 2023). Samples for dark carbon fixation were placed in a black dry bag to prevent light exposure.

After incubation, samples were terminated by acidification with TCA and then passing through a 25 mm 0.2 μm polycarbonate filter under gentle vacuum pressure (< 7 in Hg) to avoid microbial cell breakage. Filters were incubated with 0.5 mL of 3 N HCl on a heating plate set at ~60°C for ~8 hours until dry to remove any unincorporated inorganic carbon and were then amended with 10 mL of Cytoscint ES Liquid Scintillation Cocktail. Labeled particulate matter retained on the filter was used to determine the proportion of primary production incorporated into particulate carbon biomass. The filtrate was retained to determine the proportion of primary production released to the dissolved organic carbon pool. Filtrate samples were amended with 6 N HCl and placed on a heating plate set at ~60°C in a fume hood to allow the filtrate to

evaporate. The dried residue was then treated as described above for the filters. Radioactivity in the samples (disintegrations per minute; DPM) was determined using a Beckman LS6000 Liquid Scintillation Counter and converted to rates of primary production in units of micrograms of carbon per liter per day (Lizotte et al. 1996, Parsons et al. 1984). Carbon was calculated per day because PPP takes place during the day when PAR is available, whereas DCF can take place during the day and night. The assumption made for this calculation was that PPP was occurring the full 12 hours (average day length), while DCF was occurring the full 24 hours.

To correct for dark carbon fixation and background in the light bottles, the DPM were determined by subtracting the dark and the killed control incubations from the light incubations. To correct for background in the dark bottles, killed control incubations were subtracted from the dark incubations. The coefficient of variation (CV = ((standard deviation/mean)*mean) among replicates was calculated for each treatment and where CV > 20%, outlying replicates were examined and removed from further calculations. Net primary production rates were calculated using the following equation (Lizotte et al. 1996, Parsons et al. 1984):

$$\frac{DPM(l) - DPM\ (k)\ x\ (a)\ x\ (b)\ x\ (c)}{(A_{14C})\ x\ \left(\frac{Vol\ 14_C\ (\mu l)}{c}\right) x\ \left(\frac{2.2x10^6\ dpm}{1\ \mu Ci}\right)\ x\ (t)}\ x\ \frac{24\ h}{d} = \mu g\ Cl^{-1}d^{-1}$$

where DPM(l) is the average DPM of live samples, DPM(k) is the DPM of the killed control, a is the concentration of dissolved inorganic carbon, b is the isotopic discrimination factor of ^{14}C radiolabeled carbon (1.06), c is a constant to convert units (1000), A_{14C} is the specific activity of the ^{14}C, and t is the incubation period (h). The extracellular release in the filtrate was corrected similarly as described above for the determination of net primary production except the DPMs from the filtrate were used. By using the DPMs of the filtrate, the DOC within the filtrate can be calculated using the above equation. Results of DOC production were described as the percent extracellular release of total primary production (POC+DOC) that was released as DOC (Fogg et al., 1965).

2.4.3 Chloramphenicol Validation Experiments

A pilot experiment was performed on 21 October 2021 to determine an effective concentration of chloramphenicol: 5 µg ml^{-1}, 10 µg ml^{-1}, or 15 µg ml^{-1} (final concentration). This range was selected based on published literature (Brock 1961). Chloramphenicol validation experiments were conducted in triplicate. ^{14}C-bicarbonate (0.1 µCi ml^{-1} final concentration) was added to triplicate polycarbonate bottles containing 10 ml of sample water and incubated for ~ 6 hours in four treatments: control (0 µg ml^{-1}), treatment 1 (5 µg ml^{-1}), treatment 2 (10 µg ml^{-1}), treatment 3 (15 µg ml^{-1}), and a killed control for each treatment. Ice cold 100% TCA (5% final concentration) was added to the killed control treatments and placed on ice for 10-15 minutes. After incubation, samples were first acidified and then filtered through a 3.0 µm polycarbonate filter under gentle vacuum pressure (< 7 in Hg). The filters were then treated as described above for the determination of rates of photosynthetic primary productivity and dark carbon fixation. Three t-tests with unequal variances were conducted between the control + 5 µg ml^{-1} ($p=0.027$), control + 10 µg ml^{-1} ($p=0.0033$), and control + 15 µg ml^{-1} ($p=0.0008$). Another three t-tests with unequal variances were conducted between the final concentrations of chloramphenicol: 0 µg ml^{-1} + 5 µg ml^{-1}, 5 µg ml^{-1} + 10 µg ml^{-1}, and 10 µg ml^{-1} + 15 µg ml^{-1}. There was a significant difference between 0 µg ml^{-1} + 5 µg ml^{-1} ($p=0.027$), however there were no significant differences between 5 µg ml^{-1} + 10 µg ml^{-1} ($p=0.47$) and 10 µg ml^{-1} + 15 µg ml^{-1} ($p=0.56$). The concentration used in the chloramphenicol treatments was 10 µg ml^{-1} final concentration.

2.4.4 Size Fractionation Incubations

To determine whether picoplankton (0.2 to 3 µm) or microbial groups larger than 3 µm were major contributors to carbon fixation, a size fractionation experiment was conducted during the open water period (16 October 2022) and the ice covered period (11 January 2023). Incubations for net photosynthetic primary production and dark carbon fixation were conducted in triplicate. 3 µL of ^{14}C-bicarbonate (0.1 µCi ml^{-1} final concentration) was added to triplicate polycarbonate bottles containing 30 ml of sample water and incubated for ~12 hours at *in situ* temperatures in a lighted incubator as described above. Three treatments were conducted: light (photosynthetic primary

production; as close to *in situ* light as possible), dark (dark carbon fixation), and a killed control that was filtered prior to incubations to remove any microorganisms larger than 0.2 µm from samples. After incubation, samples were first filtered through a 3.0 µm polycarbonate filter under gentle vacuum pressure (< 7 in Hg). The newly collected filtrate was then passed through a 0.2 µm filter under the same vacuum pressure. The filters were then treated as described above for the determination of rates of photosynthetic primary productivity and dark carbon fixation associated with each size fraction. Results from the size fractionation experiments were described as the percent of total primary production (0.2 – 3.0 µm + > 3 µm) that was in the > 3 µm size fraction.

2.5 Statistical Analyses

Relationships between physical (ice thickness, snow depth, water temperature), chemical (SRP, TDN, DO), and biological (PPR) parameters were analyzed using nonparametric tests described below. To understand the dynamics of photosynthetic primary production and dark carbon fixation (Objective 1), a Spearman Correlation was used to assess the individual relationships between environmental conditions (ice thickness, snow depth, water temperature, SRP, TDN, DOC and DO) and PPR. To understand which environmental conditions influenced PPR, a generalized linear model (GLM) was used. The best and simplest model with the lowest Akaike Information Criterion (AIC) was selected to describe the relationships between light or dark primary production and environmental parameters. Overall model fit was indicated by R^2 value, 1 – (residual deviance / null deviance). To address objective 2, Wilcoxon paired tests with unequal variances were conducted between PPP and PPP + chloramphenicol and DCF and DCF + chloramphenicol to determine whether prokaryotic or non-prokaryotic groups made relatively greater contributions to carbon fixation during ice cover. I expected chloramphenicol treatments to be significantly lower than untreated samples if prokaryotic activity is important in carbon fixation during ice cover. Statistical analyses were conducted using the R software package (v4.1.2; R Core Team 2021).

3 Results

3.1 Physical and Chemical Conditions

During 2021, the first ice thickness measurement was recorded on 30 January. Ice thickness measured at 12 cm and had a steady increase reaching a maximum of 29 cm on 20 February. Ice thickness began to decrease for the rest of the 2021 ice covered period, until ice-off which occurred the week of 27 March. When measurements began in 2022, ice thickness was 30 cm on 8 January and increased to 43 cm on 13 January (the maximum for the season). Ice thickness ranged from 20 cm to 33 cm from 20 January until ice-off which occurred the week of 7 April.

Snow depth was first recorded on 05 February 2021 and measured 25 cm. On 13 February, snow depth reached the maximum of 45 cm and slowly began to decrease for the rest of ice cover in 2021. In 2022, snow depth was 5 cm during the first two weeks of January. Snow depth increased to 30 cm the week of 20 January. The range of snow depth was between 29 to 43 cm from 20 January to 8 March. Snow depth began to decrease on 24 February for the rest of ice cover in 2022.

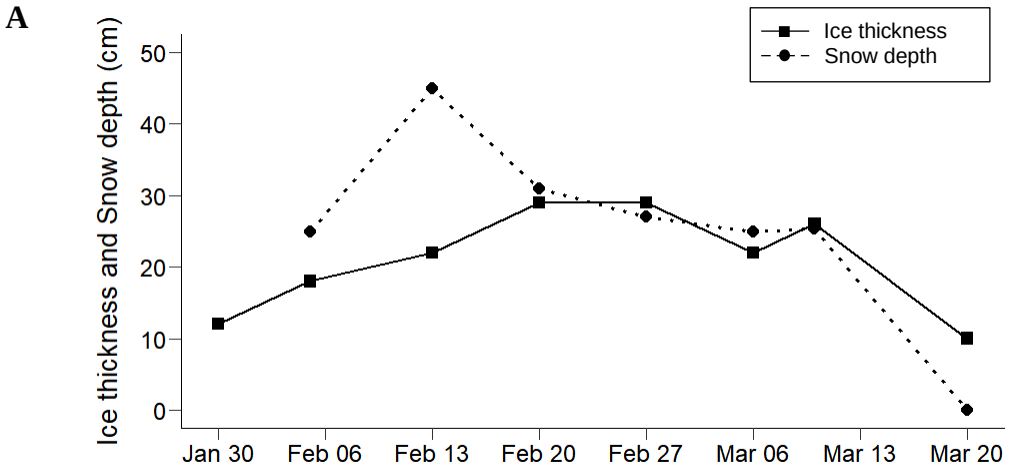

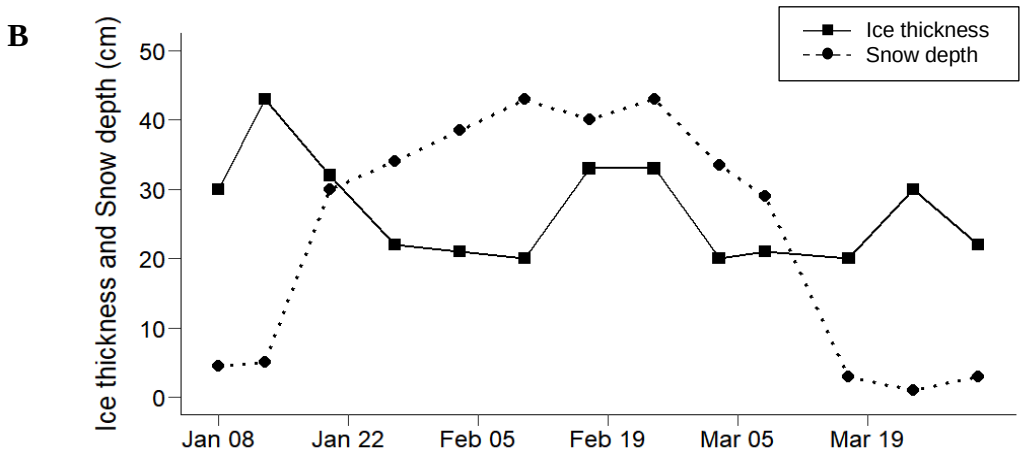

Figure 3: Ice thickness (cm) and snow depth (cm) in 2021 (A) and 2022 (B).

PAR during ice cover in 2021 ranged between 0.07 and 27.05 µmol photons m^{-2} s^{-1}. In 2022, *in situ* PAR ranged between 0.54 and 18.78 µmol photons m^{-2} s^{-1}. Samples were placed in an incubator chamber starting 30 June 2021. PAR during the open water period was substantially greater than the ice covered period. In the open water period, PAR in 2021 ranged between 12 and 223 µmol photons m^{-2} s^{-1}, while PAR in 2022 ranged between 39 and 362 µmol photons m^{-2} s^{-1}.

During ice cover in 2021, water temperatures ranged between 0.08 and 0.95°C with an average of 0.42°C (s.d.=0.31). At the beginning of ice cover in 2021, the first water temperature recorded was 0.47°C. At the beginning of March, water temperatures began to increase as the ice and snow melted. During ice cover in 2022, water temperatures ranged between 0.25 and 4.57°C with an average of 1.41°C (s.d.=1.23). Water temperatures during the open water period were greater than the ice covered period. In 2021, water temperatures ranged between 1.41°C and 23.15°C, while water temperatures in 2022 ranged between 1.13°C and 20.10°C.

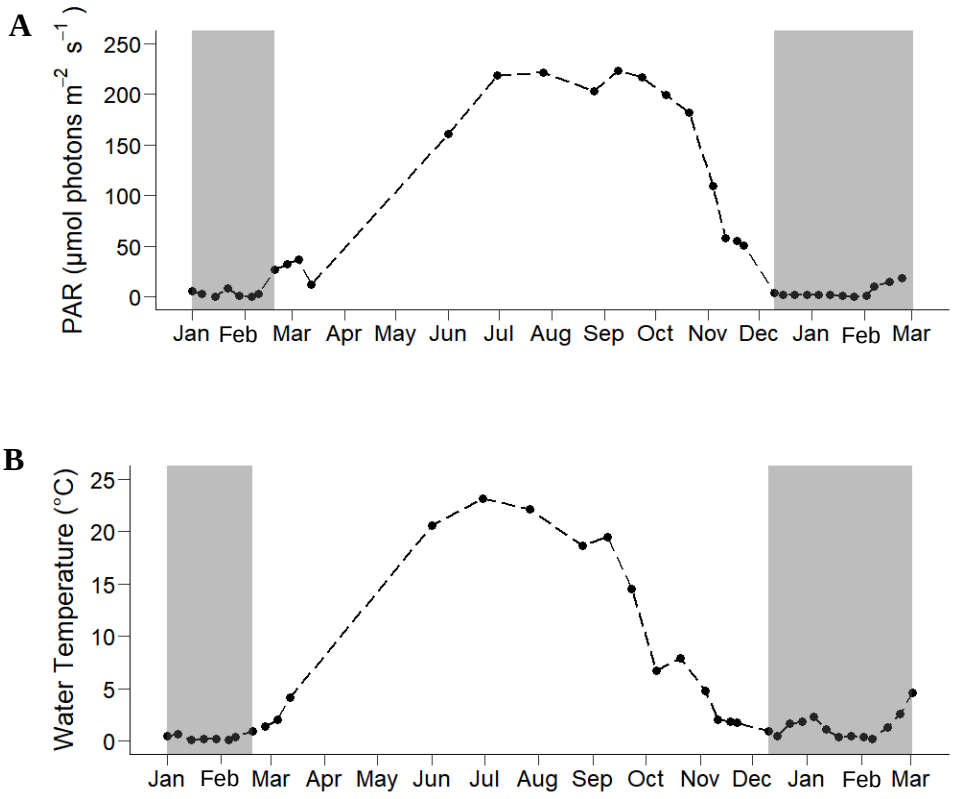

Figure 4: PAR µmol photons m^{-2} s^{-1} (A) and water temperature °C (B). Ice cover is shown in gray. Note that PAR in 2021 was recorded under ice at the time of sampling, while PAR in 2022 was recorded under ice at solar noon, Hence, 2022 represents an approximation of maximum daily PAR, while 2021 shows an *in situ* condition at the time of sampling.

In 2021, SRP concentrations started at 0.0027 mg P L^{-1} on 30 January. This was followed by a drop reaching the lowest concentration of 0.0004 mg P L^{-1} on 13 February. SRP concentrations increased for the rest of ice cover from 27 February to 10 April. In 2022, SRP concentrations started at 0.0013 mg P L^{-1} on 8 January. SRP reached its lowest concentration of 0.0004 mg P L^{-1} on 27 January. Average SRP concentrations in January 2021 (average: 0.0025 mg P L^{-1}, s.d.=0.0002) were ~1.5 times higher compared to concentrations in January 2022 (average: 0.0017 mg P L^{-1}, s.d.=0.0011). The 2021 averages for February (average: 0.0010 mg P L^{-1}, s.d.=0.0007) and March (average: 0.0026 mg P L^{-1}, s.d.=0.0012) than those of 2022 (February average: 0.0019 mg P L^{-1},

s.d.=0.0007; March average: 0.0036 mg P L^{-1}, s.d.=0.0012). SRP concentrations were greater during the ice covered period compared to the open water period. Overall, SRP concentrations were similar between the two years, ranging between 0.0002 – 0.0034 mg P L^{-1} in 2021 and 0.0006 – 0.0039 mg P L^{-1} in 2022.

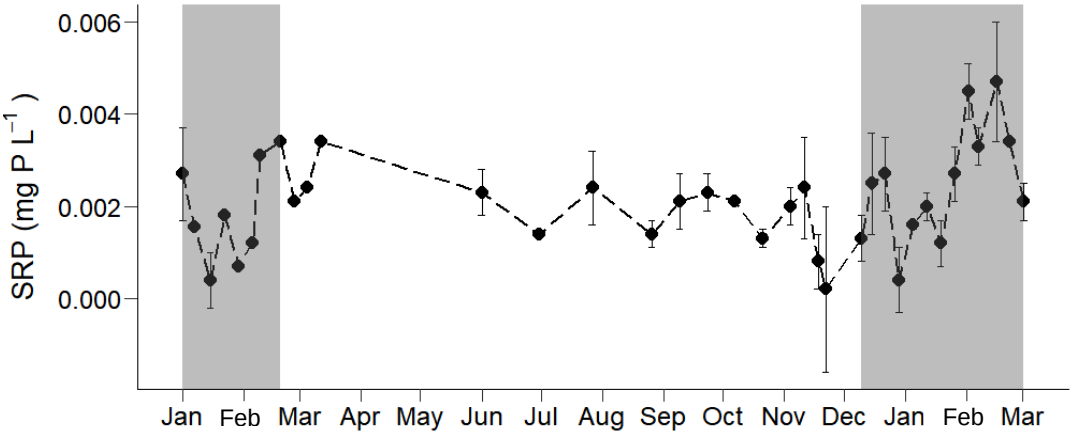

Figure 5: SRP mg P L^{-1} in the Keweenaw Waterway. Ice cover is shown in gray.

Dissolved organic carbon (DOC) and total dissolved nitrogen (TDN) measurements used in this study started on 25 August 2021. DOC was 2.085 mg C L^{-1} on 25 August and dropped to 1.293 mg C L^{-1} on 12 September. From 8 October to 17 December, DOC began to slowly decrease. During ice cover, DOC ranged between 1.163 and 1.769 mg C L^{-1} from 8 January to 31 March. TDN was at 0.299 mg N L^{-1} on 25 August. TDN concentrations increased to 0.440 mg N L^{-1} on 12 September then dropped on 8 October reaching concentrations of 0.177 mg N L^{-1}. TDN concentrations overall began to increase from 8 October to 21 December. TDN concentrations during ice cover ranged between 0.437 and 0.514 mg N L^{-1}.

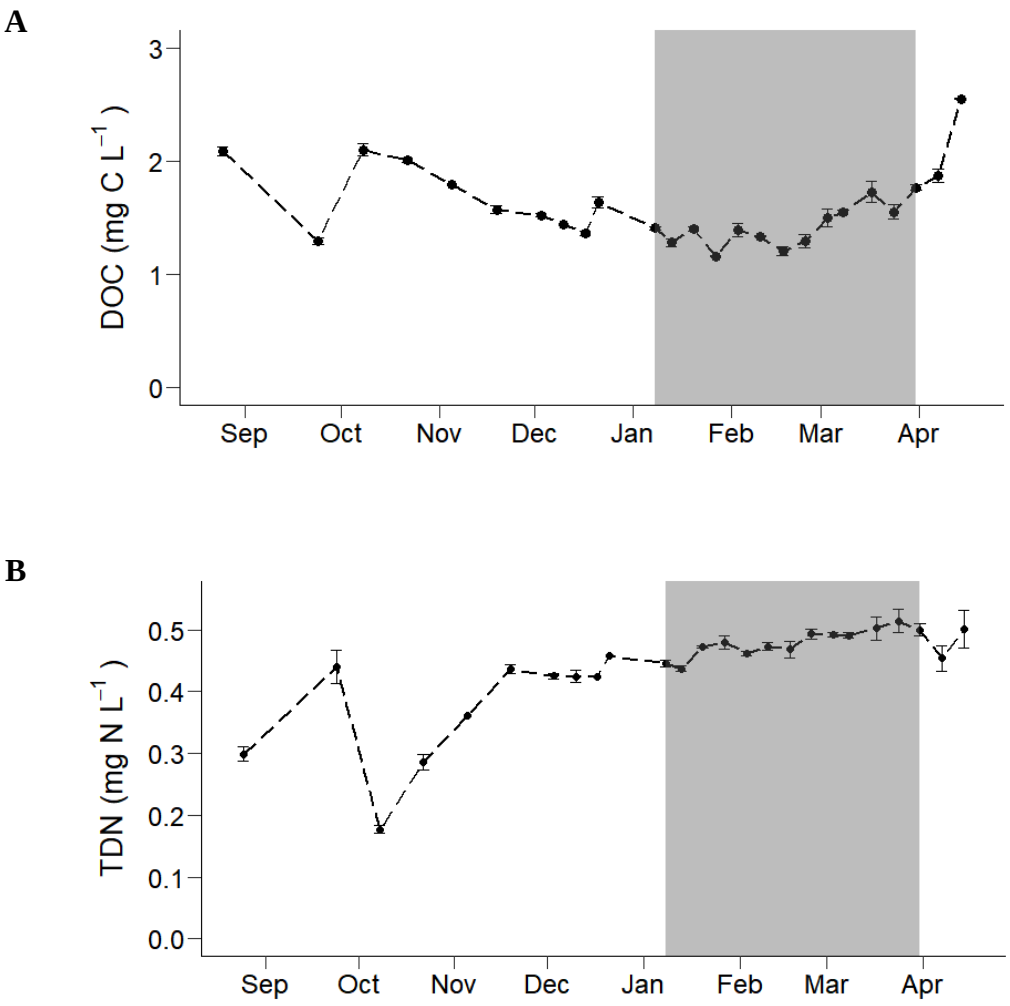

Figure 6: DOC (mg C L^{-1}) (A), and TDN (mg N L^{-1}) (B) from the open water period to ice cover in 2022. Ice cover is shown in gray.

3.2 Primary Production and Chlorophyll-a

In 2021, DCF was greater than PPP from 5 February until the week of 27 February. PPP increased from 0.026 to 0.201 µg C L^{-1} day^{-1} from 21 February to 27 February exceeding DCF. Rates of PPP ranged between 0.021 and 2.290 µg C L^{-1} day^{-1}, while rates of DCF ranged between 0.075 and 0.300 µg C L^{-1} day^{-1}. The lowest primary production rate for both PPP and DCF occurred on 13 February when snow depth was at its maximum of 45 cm. Since samples for PPP were placed in an incubator chamber that

year, samples were exposed to higher and more consistent levels of PAR. Therefore, we treat the 2022 rates as maximum estimates. Primary production rates greatly increased during the open water period.

During the open water period, PPP in 2021 ranged between 0.289 and 114.545 µg C L^{-1} day^{-1}, while rates in 2022 ranged between 2.481 and 54.766 µg C L^{-1} day^{-1}. In 2021, DCF during the open water period ranged between 0.024 and 1.638 µg C L^{-1} day^{-1}, while rates in 2022 ranged between 0.039 and 1.426 µg C L^{-1} day^{-1}.

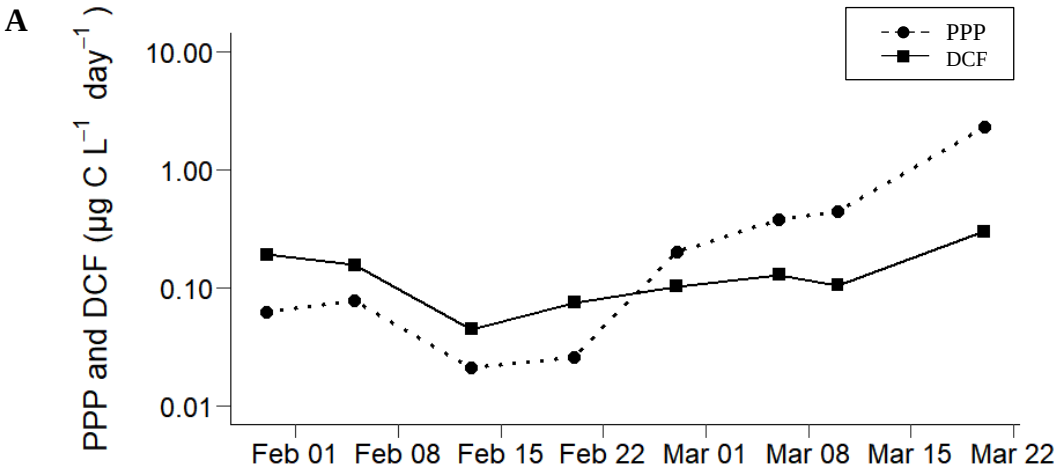

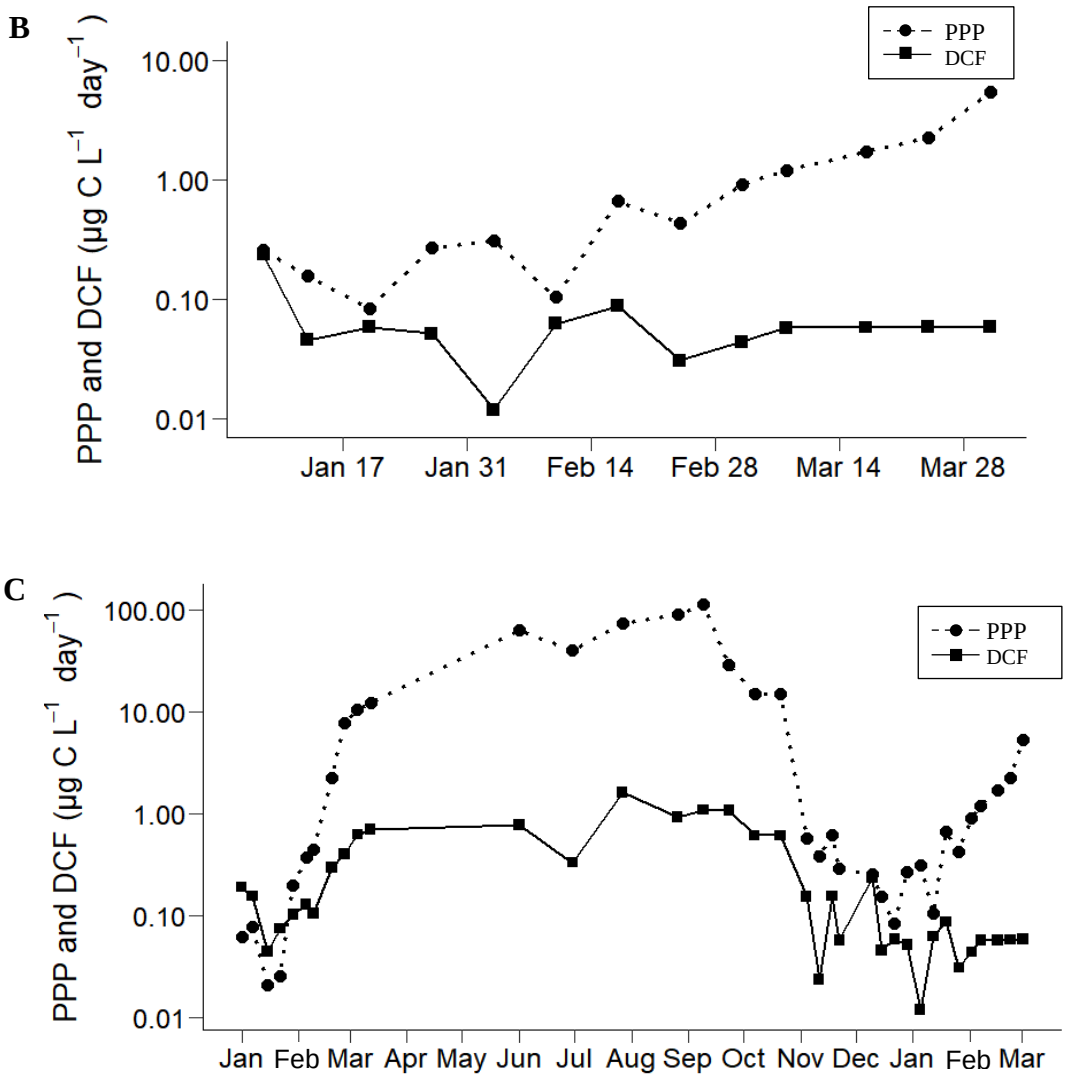

Figure 7: PPP µg C L^{-1} day^{-1} and DCF during ice cover in 2021 (A) and 2022 (B) and the open water period (C). Note the log scale for y axes.

Chlorophyll-a concentrations between 2021 and 2022 were very similar. The chlorophyll-a concentrations in 2021 ranged between 0.10 and 0.39 mg L^{-1} with an average of 0.213 mg L^{-1} (s.d.=0.09), while concentrations in 2022 ranged between 0.13 and 0.58 mg L^{-1} with an average of 0.239 mg L^{-1} (s.d.=0.11). In both years, two peaks were observed during ice cover. In 2021, the first peak occurred on 13 February and the second peak occurred on 6 March, while the first peak in 2022 occurred on 27 January and the second peak occurred on 3 March. Similar to PPP, chlorophyll-a concentrations

are higher during the open water period compared to the ice covered period. Chlorophyll-a concentrations in 2021 ranged between 0.20 and 3.95 mg L^{-1}, while concentrations in 2022 ranged between 1.03 and 4.51 mg L^{-1}.

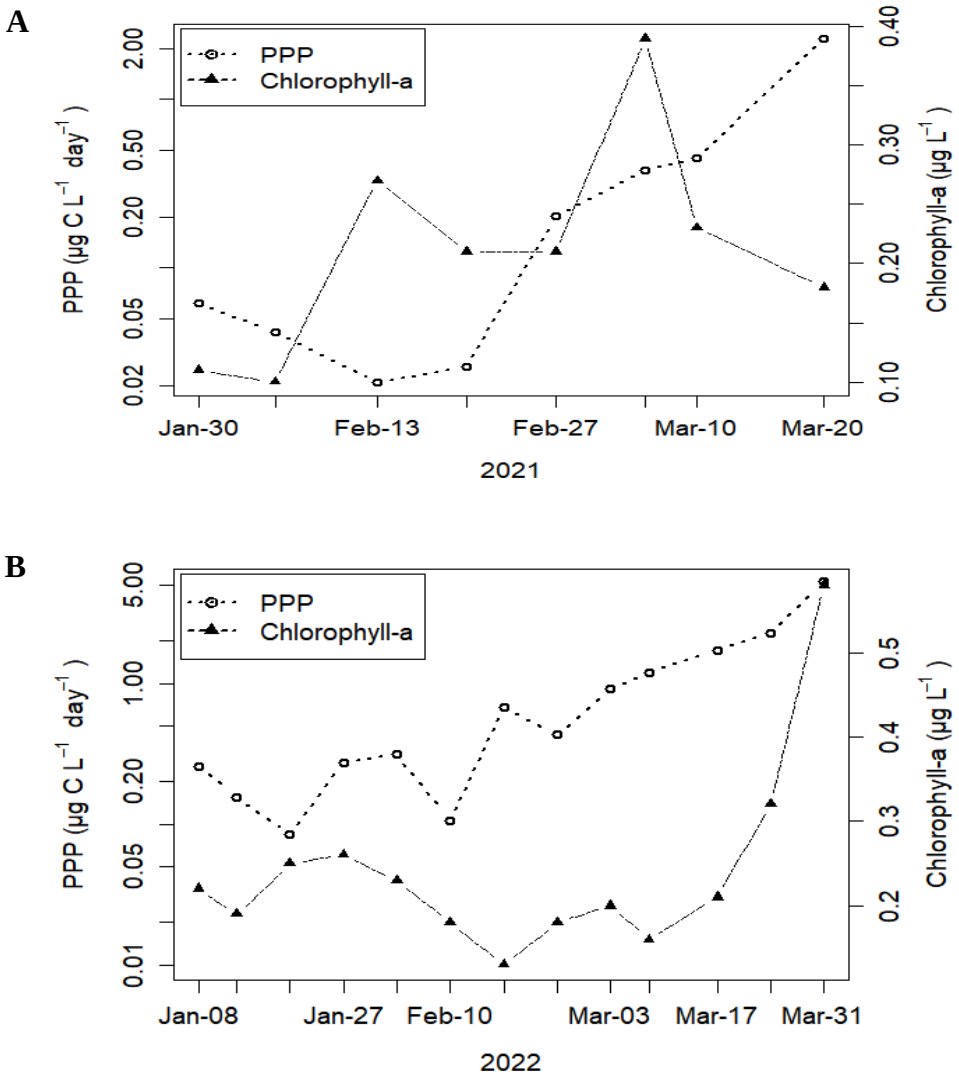

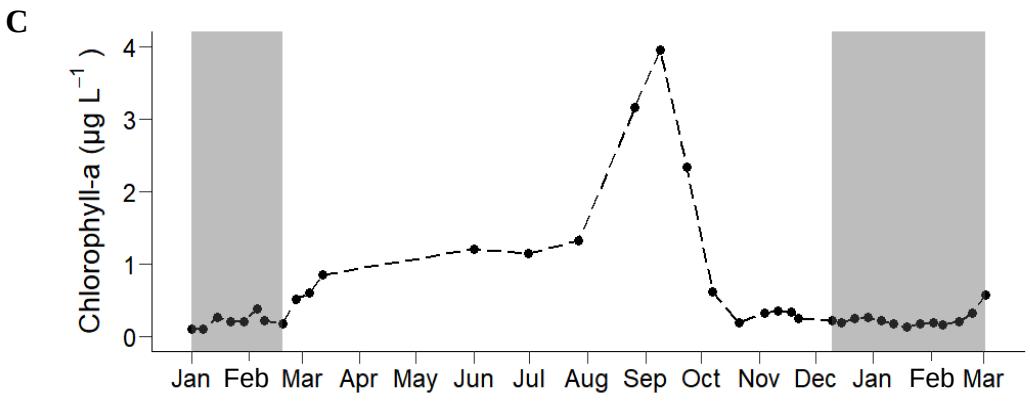

Figure 8: Chlorophyll-a and PPP from ice cover 2021 (A) and 2022 (B). Note the log scale for y axes. Chlorophyll-1 during the open water period (C). Ice cover is shown in gray.

3.3 Correlation Between Primary Production Rates and Environmental Conditions

Results of Spearman Rank Correlation analyses are shown in Table 2 (data from 2021 and 2022). Correlations were between environmental conditions (water temperature, snow depth, DOC, DO, conductivity, and TDN) to PPR (PPP, DCF). All correlations were statistically significant except for the correlations between DOC and PPP (Spearman; r= 0.36, p=0.08) and between TDN and PPP (Spearman; r= -0.32, p=0.12).

Table 2: Results of Spearman Correlation between environmental conditions and PPP and DCF. Significance (α=0.05).

Environmental conditions	**PPP**	**DCF**
	(r-value, p-value)	(r-value, p-value)
Water temperature	(0.50, 8.0×10^{-4})	(0.62, 9.93×10^{-6})
Snow depth	(-0.49, 0.029)	(-0.48, 0.03)
DOC	(0.36, 0.08)	(0.58, 0.0025)
DO	(-0.48, 0.0014)	(-0.75, 1.50×10^{-8})
Conductivity	(0.37, 0.02)	(0.71, 4.58×10^{-7})

Environmental conditions	PPP	DCF
	(r-value, p-value)	(r-value, p-value)
TDN	(-0.32, 0.12)	(-0.48, 0.02)

In addition to the Spearman Rank correlation, generalized linear models (GLM) were used to determine the relationships between environmental parameters and PPR (PPP, DCF) in 2022, with the goal being to determine whether there are environmental conditions that influence PPR more than others. The best model (determined as the simplest model that minimized AIC) for PPP included snow depth, water temperature, DO, DOC, and conductivity. The best model for DCF included snow depth, water temperature, TDN, DO, DOC, and conductivity. The R^2 value was calculated using the null and residual deviance. The R^2 for the PPP model was 0.81, while the R^2 for the DCF model was 0.86. Together, these data from 2022 suggest that snow depth, water temperature, DO, DOC, and conductivity were important influencing PPP, while snow depth, water temperature, TDN, DO, DOC, and conductivity were important in influencing DCF.

Table 3: Results of GLM for PPP and DCF in 2022. Significance (α=0.05).

Environmental conditions	PPP	DCF
	(r-value, p-value)	(r-value, p-value)
Snow depth	(-0.0290, 0.356)	(-9.30×10^{-4}, 0.515)
Temperature	(0.938, 0.146)	(0.00507, 0.822)
TDN		(0.325, 0.712)
DO	(0.727, 0.456)	(0.0141, 0.704)
DOC		(-0.0573, 0.632)
Conductivity	(-0.0250, 0.478)	(0.00541, 0.00828)

3.4 Primary Contributors to Wintertime Carbon Fixation

To address whether prokaryotic or non-prokaryotic groups were the primary contributors to wintertime carbon fixation, chloramphenicol was added, a prokaryotic inhibitor, to the PPP and DCF incubations during the ice-covered period of 2022. Wilcoxon paired tests were used to compare rates in treatments amended with chloramphenicol to those with no amendment. The chloramphenicol treatments were not significantly different (α=0.05) from the treatments with no amendment for PPP (Wilcoxon paired test; V=24, p=0.46, n=9) or DCF (Wilcoxon paired test; V=23, p=0.5, n=9). This suggests prokaryotic groups were not affected by the chloramphenicol treatments.

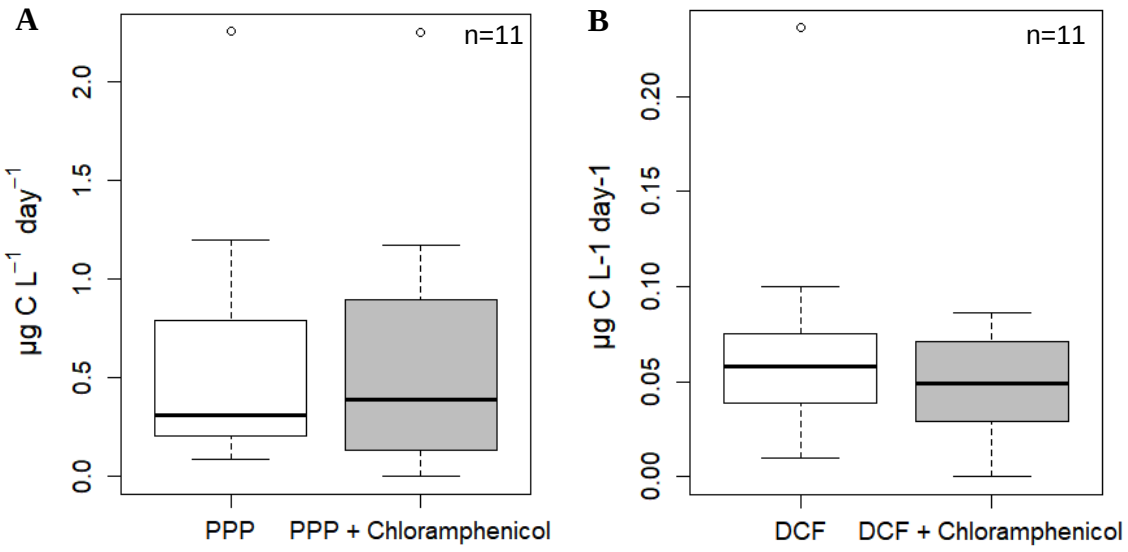

Figure 9: Chloramphenicol treatments during ice cover in 2022. PPP and PPP with chloramphenicol (A) and DCF and DCF with chloramphenicol (B).

Because it is possible that organisms in the samples were resistant to chloramphenicol, size fractionation experiments were also conducted on 26 October 2022 (open water period) and 11 January 2023 (ice covered period) to further assess whether the primary contributors to carbon fixation could be divided into different guilds. The assumption associated with this approach is that photosynthetic primary producers (e.g.,

cyanobacterial filaments, diatoms) are likely larger chemosynthetic primary producers (e.g., unicellular bacteria or archaea).

PPP was ~ 4.4 times higher in the larger size fraction during the open water period, while primary production rates varied little between size fractions during the ice cover period. DCF rates determined in these experiments were similar across open water and ice covered periods. Compared to the rest of the data set, both of these incubations represented relatively low rates of production. For example, rates in October 2021 were ~ 65 times higher than the summed size fractions in the October 2022 experiment. This suggests that this incubation may not be representative of the whole data set.

Table 4: Size fractionation during the open water (26 October 2022) and ice covered (11 January 2023) period. The standard deviation (s.d.) is shown on the right.

Treatment	PPP (+/- s.d.) (μg C L^{-1} day^{-1})	DCF (+/- s.d.) (μg C L^{-1} day^{-1})
Open water period		
0.2 – 3.0 μm	0.080 (0.005)	0.014 (0.012)
> 3.0 μm	0.354 (0.030)	0.021 (0.026)
Ice covered period		
0.2 - 3.0 μm	0.015 (0.009)	0.006 (0.009)
> 3.0 μm	0.020 (0.013)	0.006 (0.004)

3.5 The Partitioning of Dissolved Organic Carbon Versus Particulate Organic Carbon

PPP had lower extracellular release of DOC when compared to the extracellular release associated with DCF. Data points indicating 0% DOC production in Figure A and B were from the killed control treatments being higher than the light/dark treatments. When the light/dark treatments were above the killed control treatments, the extracellular release of DOC associated with DCF and DCF + chloramphenicol were mostly between 27% and 97% μg C L^{-1} day^{-1}, while the extracellular release of DOC associated with PPP and PPP + chloramphenicol were spread out between 30% and 62% μg C L^{-1} day^{-1}.

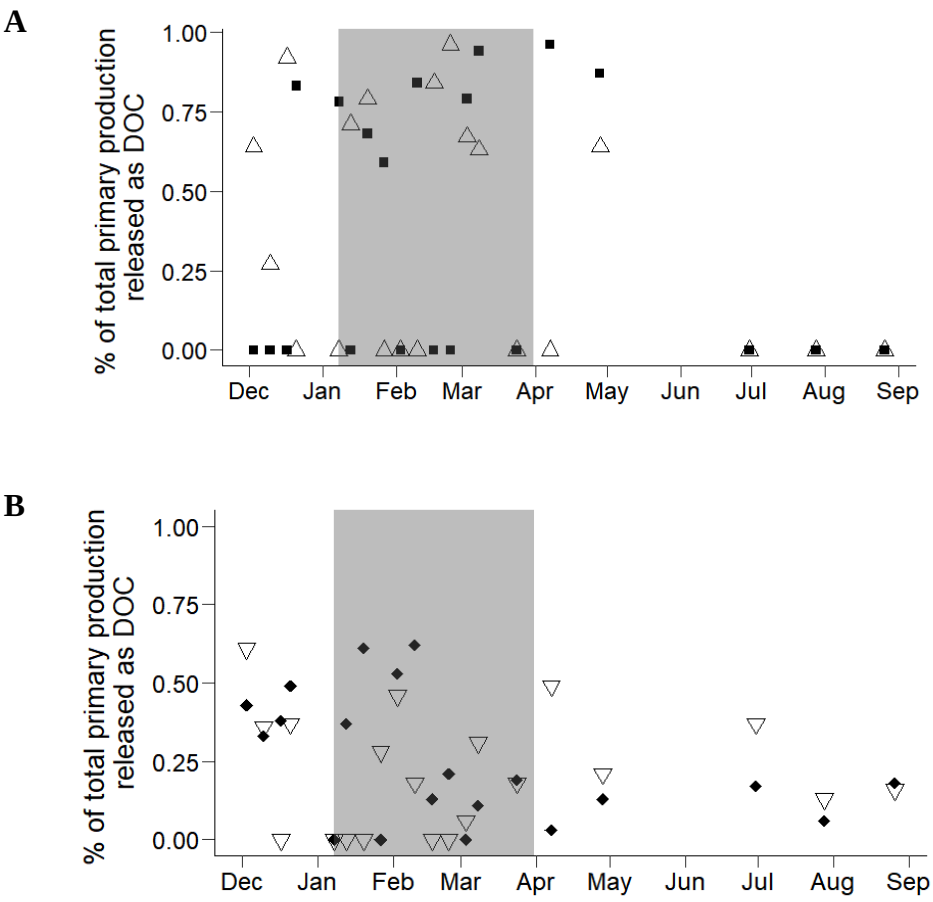

Figure 10: Total primary production released as DOC for DCF, DCF + chloramphenicol (A) and PPP, PPP + chloramphenicol (B). The ice covered period is shown in gray.

4 Discussion

In this study, the dynamics of PPP and DCF were analyzed, along with their relationships with various environmental conditions. The results of this study revealed PPP and DCF were suppressed during the ice covered period compared to the open water period, supporting previous work that suggests ice cover heavily influences PPR. This study also determined primary contributors to wintertime carbon fixation based on size (as a proxy for guild membership) and the partitioning of organic carbon (dissolved vs the particulate fraction).

4.1 Primary Production Rates (PPR)

4.1.1 Ice Thickness and Snow Depth: Controls on PPR

Climate change is causing fluctuations in ice and snow cover (Magnuson et al. 2000, Brown and Mote, 2009). These fluctuations can change ecosystem dynamics, starting at the base of the food chain. For example, years of high ice and snow cover can reduce PAR penetration for photoautotrophs, ultimately decreasing productivity in the ecosystem. The Keweenaw Waterway experienced more ice and snow cover in 2022 compared to 2021. On average, ice thickness and snow depth were ~ 1.5 times and ~ 1.7 times greater, respectively, in 2022 than 2021. Overall, PPP and DCF decreased while ice thickness and snow depth increased. The lowest rates of PPP occurred during the maximum snow depth of 45 cm. Snow cover can be a major determinant of how much PAR can reach the water column (Jewson et al. 2009) and control phytoplankton blooms under the ice. Once snow depth began to decrease, PPP slowly increased under the ice despite a slow increase in ice thickness. This suggests snow depth played a larger part in regulating PPP compared to ice thickness. PPP quickly increased in mid-March as snow depth and ice thickness both decreased.

DCF followed a similar pattern to PPP; however, DCF was greater than PPP on a daily basis at the beginning of ice cover until the end of February in 2021, suggesting DCF can be an essential source of wintertime carbon fixation. Since samples for PPP and DCF were placed in an incubator chamber in 2022, ice thickness and snow depth did not directly influence primary production rates determined in the experiments; however,

incubations were conducted as close to natural maximum PAR as possible, and samples were taken from the natural environment. Therefore, ice and snow cover would still be expected to influence the community composition of photoautotrophs and chemoautotrophs in the experiments. Primary production rates in 2022 overall followed similar patterns to those of 2021 where primary production rates decreased with increasing ice and snow cover.

4.1.2 PAR and Water Temperature: Controls on PPR

PPP is reduced by low levels of PAR, often limiting the growth of photoautotrophs. The minimum amount of PAR needed to sustain photosynthetic growth has been estimated to be 10 μmol photons m^{-2} s^{-1} (Raven et al. 2000), while another study estimated the minimum requirement to be 0.36 μmol photons m^{-2} s^{-1} (Mock and Gradinger 2000). PAR in the Keweenaw Waterway was well below the minimum PAR required by Raven et al (2000) and closer to the minimum PAR required by Mock and Gradinger (2000). The minimum PAR measured in 2021 was 0.07 μmol photons m^{-2} s^{-1} on 13 February, however, PAR in 2021 was determined at the time of sample collection (near sunrise), meaning the 2021 PAR values capture a minimal level of PAR. Because ice thickness and snow depth were greater in 2022, I would expect that PAR would have been higher in 2021 and lower in 2022. When limited by the availability of PAR, some photoautotrophs can increase their chlorophyll-a content to maximize their ability to capture PAR to support photosynthesis under ice ("photoadaptation" e.g., Felip and Catalan 2000, Morgan-Kiss et al. 2016), supporting the maintenance of PPP even with high ice thickness or snow cover. This is a possible explanation for the chlorophyll-a concentrations observed in the Keweenaw Waterway, which increased during ice cover in 2021 and 2022, suggesting possible photoadaptation. Additionally, studies have shown motility to be a key trait for phytoplankton communities under ice, as phytoplankton can migrate to photic zones (Henshaw and Laybourn-Parry 2002, Rue et al. 2020). Because our samples were collected near the surface of the water column (1 m), it is possible that increases in chlorophyll-a concentrations also resulted from upward migration of phytoplankton in response to low levels of PAR.

PAR in 2022 was determined at solar noon the day before sample collection to estimate the maximum potential PAR associated with each incubation period. Samples were then incubated in a lighted incubator exposed to low levels of PAR to simulate the effect of ice and snow cover. The lowest possible PAR setting in the incubator exceeded *in situ* PAR determined prior to sampling, thus the PPP rates determined here likely represent maximal estimates, assuming that PPP is light-limited. Since DCF relies on chemical energy to regulate their metabolism, I expected PAR to have little to no effect on DCF. PPP was ~ 2 times greater in 2022 compared to 2021, while for DCF the opposite was true: rates were ~1.7 times lower in 2022 compared to 2021.

In situ water temperatures in 2022 were ~ 3 times higher than that of 2021, on average. Lower temperatures are generally associated with slower rates of metabolic activity. Since water temperatures in 2021 (average = 0.42°C, s.d.=0.31) were lower compared to 2022 (average = 1.41°C, s.d.=1.23), this may partially explain why PPP was lower in 2021 than 2022, whereas the higher water temperatures in 2022 may be part of the reason why PPP was higher. Incubation temperatures (average = 1.65°C, range = 1°C – 4.57°C) in 2022 were elevated relative to water column temperatures (average = 1.41°C, range = 0.25 – 4.57°C), due to the limited lower temperature range in the incubator, which could have further elevated the observed rates.

4.1.3 Nutrients: Controls on PPR

Phosphorus is a key nutrient for microbial growth that can be limited in many freshwater ecosystems including Lake Superior (Sterner et al. 2004). Despite low concentrations of SRP in the Keweenaw Waterway in 2021 and 2022, concentrations increased during ice cover in both years. Increases in SRP concentrations around the time of ice off can partially be explained by the additional nutrients within the ice that enter the water column as ice begins to melt (Yang et al. 2021) and nutrients that are flushed in from land as snow melts. However, the increase in nutrient concentrations during ice cover is expected as heterotrophic organisms regenerate nutrients while photosynthetic demand is depressed. Maximum SRP concentrations during ice cover 2021 were 0.0034 mg P L^{-1} on 20 March, while maximum concentrations during ice cover 2022 were

0.0047 mg P L^{-1} (s.d.=0.0013) on 17 March. Both of these maximum SRP concentrations were well above the maximum during the open water period (0.0024 mg P L^{-1} two year max).

Nitrate has also been found to accumulate during ice cover (Hampton et al. 2017). High nitrate concentrations may be a result of chemoautotrophs carrying out nitrification with nitrate being the end product (Powers et al. 2017). Since TDN (average= 34.202 μmol N L^{-1}, s.d.= 1.602) is greater than SRP (average: 0.077 μmol P L^{-1}, s.d.= 0.042), this yields a high N:P ratio compared to the Redfield N:P ratio. This ratio is important for microbial assimilatory (build biomass) and dissimilatory (capture energy) processes. Stoichiometry ratios like N:P are also useful in understanding the composition and growth of microbial groups (Wetzel 2001). Both TDN and SRP were low during the open water period and increased heading into the ice covered period. The average N:P ratio during ice cover was 442.89 μmol, while during the open water period it was 411.62 μmol. This indicates the N:P ratio is higher during the ice covered period compared to the open water period which could potentially alter the community structure.

4.1.4 Primary Contributors to Wintertime Carbon Fixation

To determine whether prokaryotic or non-prokaryotic groups are primary contributors to wintertime carbon fixation, chloramphenicol was added as an additional treatment to PPP and DCF incubations. Chloramphenicol is a broad-spectrum antibiotic that inhibits prokaryotic protein synthesis by binding to the 50S portion of the ribosome and preventing the formation of polypeptide bonds (Dinos et al. 2016). The use of chloramphenicol is inexpensive and efficient at suppressing rates of protein synthesis in prokaryotic communities (Agostini et al. 2019). Like all microbial inhibitors, there may be some bacterial and archaeal groups that are resistant to chloramphenicol, or that require higher concentrations of chloramphenicol to inhibit protein synthesis. Treatments amended with chloramphenicol were expected to decrease DCF driven by chemoautotrophs; however, on average, results showed no significant difference between DCF + chloramphenicol and DCF treatments (Wilcoxon paired test; V=23, p=0.5, n=9). Since cyanobacteria are members of the domain Bacteria, chloramphenicol treatments

could also lower rates in PPP that are partly driven by cyanobacteria, however, the abundance of cyanobacteria in this study is unknown. Results from this experiment indicated chemoautotrophs sensitive to chloramphenicol were not major contributors to carbon fixation during ice cover in 2022. While archaea are expected to be influenced by chloramphenicol, some have been shown to be resistant (Khelaifia et al. 2012). Given that the abundance of archaea was found to increase during ice cover in the Keweenaw Waterway, while the abundance of bacteria decreased (Butler et al. 2019), it is possible that archaea conducting DCF were not inhibited by chloramphenicol treatment.

Size fractionation experiments were conducted in the open water period (26 October 2022) and the ice covered period (11 January 2023) to determine whether picoplankton (0.2 to 3 µm) or microbial groups larger than 3 µm were likely to be major contributors to wintertime carbon fixation. The light treatment of the large size fraction (>3 µm) accounted for a larger proportion of total primary production during the open water period (81.6%) than the ice covered period (57.1%). DCF in the large size fraction (>3 µm) represented a higher proportion of total primary production during the open water, relative to the ice covered period (60% and 50% of respectively). These results suggest photoautotrophs larger than 3 µm were important in carbon fixation, especially during the open water period (PPP= 81.6%). Results also indicated DCF occurred in the larger size fraction during the open water period (DCF= 60%), suggesting that anapleurotic reactions (the replenishment of intermediates of the Calvin Cycle) carried out by larger, eukaryotic cells or cyanobacteria could be included in DCF. More of these experiments are needed to be able to confidently confirm these results since these experiments were only conducted once per period (ice-on and ice-off).

4.1.5 Extracellular Release of Dissolved Organic Carbon Versus Particulate Organic Carbon

Primary producers can partition organic carbon in the dissolved fraction as DOC or in the particulate fraction as POC (biomass). Depending on the environment and the available resources, microorganisms may try to conserve as much energy during limited environmental conditions (e.g., reduced PAR) therefore, I expected POC production to be

greater during the ice covered period than DOC production. POC production accounted for a greater relative proportion of PPP as expected. Extracellular release of DOC by phytoplankton has been reported to be between 5 – 35% (Fogg 1966, Sharp 1993) and the extracellular release of PPP results presented here are within that range. The same was not true for DCF, where DOC production was greater than POC production. During ice cover, the highest extracellular release of DOC associated with DCF was 94% on 8 March and DCF + chloramphenicol was reaching 96% on 24 February. After ice-off which occurred during the week of 31 March, DOC production associated with DCF and DCF + chloramphenicol stayed above 64% until 28 April. For the rest of the open water period, extracellular release associated with DCF and DCF + chloramphenicol were below the killed control treatments. Although the data is variable, extracellular release of DOC associated with PPP and PPP + chloramphenicol were observed to be below 65%, while DCF and DCF + chloramphenicol were mostly observed to be above 50% of extracellular release of DOC suggesting DCF may be an important source of DOC to the water column.

5 Conclusions

This study revealed the dynamics of PPP and DCF under the ice in the Keweenaw Waterway as well as provided insight into the importance of these processes to aquatic carbon fixation. Primary production is a major source of new organic carbon to aquatic systems. Rising atmospheric temperatures can lead to changes in ice cover and other environmental conditions (e.g., ice thickness, snow cover, water temperature, nutrients) that can heavily suppress primary production rates, as shown in this study. Photoautotrophs and chemoautotrophs responded differently during ice cover. Since photoautotrophs rely on incoming PAR as an energy source, PPP was further suppressed during ice cover while DCF still occurred during light-limited conditions. Because these microbial groups use different energy sources, this can lead to changes in the amount of organic carbon that enters the system which can affect higher trophic levels.

In addition, this study also investigated the partitioning of organic carbon into DOC or biomass production (POC). DOC is a significant portion of carbon in the carbon pool that can be cycled through heterotrophic bacteria and the microbial loop. Results from this study indicated the extracellular release of DOC associated with DCF was greater than that of PPP, suggesting DCF may be an essential source of DOC to the water column and the microbial loop. Together these results provided insight into the strategies photoautotrophs and chemoautotrophs implement during ice cover and the open water period and supported the growing knowledge of the important contribution of DCF to total primary production in aquatic systems. With ice covered lakes experiencing a decrease in ice cover, it is expected to see an increase in primary production rates. This may have an influential role in the productivity of the whole lake system, which makes this research critical to understand and can help researchers give insight into how primary producers may respond to climate change in the future.

6 Literature Cited

Agostini, V.O., Lopes, L.F.D.P., Macedo, A.J., Muxagata, E., 2019. A review on the effects of antimicrobials use in cultures of planktonic organisms: a procedure for ecological experiments. Latin American Journal of Aquatic Research 47, 394–415.

Arst, H., Erm, A., Leppäranta, M., Noorma, A., 2006. Radiative characteristics of ice-covered fresh- and brackish-water bodies. Proceedings of the Estonian Academy of Sciences. Geology 55.

Auguet, J.-C., Nomokonova, N., Camarero, L., Casamayor, E.O., 2011. Seasonal Changes of Freshwater Ammonia-Oxidizing Archaeal Assemblages and Nitrogen Species in Oligotrophic Alpine Lakes. Applied and Environmental Microbiology 77, 1937–1945.

Baehr, M.M., McManus, J., 2003. The measurement of phosphorus and its spatial and temporal variability in western Lake Superior. J. Great Lakes Res. 29, 479–487.

Block, B.D., Denfeld, B.A., Stockwell, J.D., Flaim, G., Grossart, H.F., Knoll, L.B., Maier, D.B., North, R.L., Rautio, M., Rusak, J.A., Sadro, S., Weyhenmeyer, G.A., Bramburger, A.J., Branstrator, D.K., Salonen, K., Hampton, S.E., 2019. The unique methodological challenges of winter limnology. Limnol Oceanogr Methods 17, 42–57.

Bolsenga, S.J., 1981. Radiation Transmittance through lake ice in the 400–700 nm Range. J. Glaciol. 27, 57–66.

Brock, T.D., 1961. Chloramphenicol. Bacteriological Reviews 25, 32–48.

Brown, R.D., Mote, P.W., 2009. The Response of Northern Hemisphere Snow Cover to a Changing Climate. Journal of Climate 22, 2124–2145.

Butler, T.M., Wilhelm, AC., Dwyer, A.C. et al. 2019. Microbial Community Dynamics During Lake Ice Freezing. Scientific Reports 9, 6231.

Butterwick, C., Heaney, S. I., & Talling, J. F. 2005. Diversity in the influence of temperature on the growth rates of freshwater algae, and its ecological relevance. Freshwater Biology, 50, 291–300.

Callieri, C., 2008. Picophytoplankton in Freshwater Ecosystems: The Importance of Small-Sized Phototrophs. Freshwater Reviews 1, 1–28.

Cavaliere, E., & Baulch, H. M. 2018. Denitrification under lake ice. Biogeochemistry, 137, 285–295.

Churchill, J. H., Kerfoot, W. C. & Auer, M. T. 2004. Exchange of water between the Keweenaw Waterway and Lake Superior: characteristics and forcing mechanisms. Journal of Great Lakes Research 30, 55–63.

Cota G. F. 1985. Photoadaptation of high Arctic ice algae. Nature, 315, 219–222.

Dinos, G.P., Athanassopoulos, C.M., Missiri, D.A., Giannopoulou, P.C., Vlachogiannis, I.A., Papadopoulos, G.E., Papaioannou, D., Kalpaxis, D.L., 2016. Chloramphenicol Derivatives as Antibacterial and Anticancer Agents: Historic Problems and Current Solutions. Antibiotics (Basel) 5, 20.

Dokulil, M.T., Herzig, A., 2009. An analysis of long-term winter data on phytoplankton and zooplankton in Neusiedler See, a shallow temperate lake, Austria. Aquat Ecol 43, 715–725.

Felip, M., Catalan, J., 2000. The relationship between phytoplankton biovolume and chlorophyll in a deep oligotrophic lake: decoupling in their spatial and temporal maxima. Journal of Plankton Research 22, 91–106.

Fogg, G.E. 1966. The extracellular products of algae. Oceangr. Mar. Biol. Annu. Rev. 4:195-212.

Garcia, S.L., Szekely, A.J., Bergvall, C., Schattenhofer, M., Peura, S., 2019. Decreased Snow Cover Stimulates Under-Ice Primary Producers but Impairs Methanotrophic Capacity. mSphere 4, e00626-18.

Gerten, D., Adrian, R., 2000. Climate-driven changes in spring plankton dynamics and the sensitivity of shallow polymictic lakes to the North Atlantic Oscillation. Limnology and Oceanography 45, 1058–1066.

Hampton, S.E., Galloway, A.W.E., Powers, S.M., Ozersky, T., Woo, K.H., Batt, R.D., Labou, S.G., O'Reilly, C.M., Sharma, S., Lottig, N.R., Stanley, E.H., North, R.L., Stockwell, J.D., Adrian, R., Weyhenmeyer, G.A., Arvola, L., Baulch, H.M., Bertani, I., Bowman Jr., L.L., Carey, C.C., Catalan, J., Colom-Montero, W., Domine, L.M., Felip, M., Granados, I., Gries, C., Grossart, H.-P., Haberman, J., Haldna, M., Hayden, B., Higgins, S.N., Jolley, J.C., Kahilainen, K.K., Kaup, E., Kehoe, M.J., MacIntyre, S., Mackay, A.W., Mariash, H.L., McKay, R.M., Nixdorf, B., Nõges, P., Nõges, T., Palmer, M., Pierson, D.C., Post, D.M., Pruett, M.J., Rautio, M., Read, J.S., Roberts, S.L., Rücker, J., Sadro, S., Silow, E.A., Smith, D.E., Sterner, R.W., Swann, G.E.A., Timofeyev, M.A., Toro, M., Twiss, M.R., Vogt, R.J., Watson, S.B., Whiteford, E.J., Xenopoulos, M.A., 2017. Ecology under lake ice. Ecology Letters 20, 98–111.

Henshaw, T., Laybourn-Parry, J., 2002. The annual patterns of photosynthesis in two large, freshwater, ultra-oligotrophic Antarctic lakes. Polar Biol 25, 744–752.

Hoppe, H.-G., Breithaupt, P., Walther, K., Koppe, R., Bleck, S., Sommer, U., Jürgens, K., 2008. Climate warming in winter affects the coupling between phytoplankton and bacteria during the spring bloom: a mesocosm study. Aquatic Microbial Ecology 51, 105–115.

Huang, W., Zhang, Z., Li, Z., Leppäranta, M., Arvola, L., Song, S., Huotari, J., Lin, Z., 2021. Under-Ice Dissolved Oxygen and Metabolism Dynamics in a Shallow Lake: The Critical Role of Ice and Snow. Water Resources Research 57, e2020WR027990.

Ivanikova, N.V., Popels, L.C., McKay, R.M.L., Bullerjahn, G.S., 2007. Lake Superior Supports Novel Clusters of Cyanobacterial Picoplankton. Appl Environ Microbiol 73, 4055–4065.

Jewson, D.H., Granin, N.G., Zhdanov, A.A., Gnatovsky, R.Y., 2009. Effect of snow depth on under-ice irradiance and growth of Aulacoseira baicalensis in Lake Baikal. Aquat Ecol 43, 673–679.

Jöhnk, K. D., Huisman, J., Sharples, J., Sommeijer, B., Visser, P. M., & Stroom, J. M. 2008. Summer heatwaves promote blooms of harmful cyanobacteria. Global Change Biology, 14, 495–512.

Jung, M.-Y., Sedlacek, C.J., Kits, K.D., Mueller, A.J., Rhee, S.-K., Hink, L., Nicol, G.W., Bayer, B., Lehtovirta-Morley, L., Wright, C., de la Torre, J.R., Herbold, C.W., Pjevac, P., Daims, H., Wagner, M., 2022. Ammonia-oxidizing archaea possess a wide range of cellular ammonia affinities. ISME J 16, 272–283.

Kelley, D.E., 1997. Convection in ice-covered lakes: effects on algal suspension. J Plankton Res 19, 1859–1880.

Khelaifia, S., Drancourt, M., 2012. Susceptibility of archaea to antimicrobial agents: applications to clinical microbiology. Clinical Microbiology and Infection 18, 841–848.

Kirchman, David L. Processes in Microbial Ecology. Available from: VitalSource Bookshelf, (2nd Edition). Oxford University Press Academic UK, 2018.

Kirillin, G., Leppäranta, M., Terzhevik, A., Granin, N., Bernhardt, J., Engelhardt, C., Efremova, T., Golosov, S., Palshin, N., Sherstyankin, P., Zdorovennova, G., Zdorovennov, R., 2012. Physics of seasonally ice-covered lakes: a review. Aquatic Sciences 74, 659–682.

Knowles R, Lean DRS. Nitrification: A Significant Cause of Oxygen Depletion Under Winter Ice. Canadian Journal of Fisheries and Aquatic Sciences. 1987; 44(4):743–9.

Könneke, M., Bernhard, A.E., de la Torre, J.R., Walker, C.B., Waterbury, J.B., Stahl, D.A., 2005. Isolation of an autotrophic ammonia-oxidizing marine archaeon. Nature 437, 543–546.

Lemke, P., J. Ren, R.B. Alley, I. Allison, J. Carrasco, G. Flato, Y. Fujii, G. Kaser, P. Mote, R.H. Thomas and T. Zhang, 2007: Observations: Changes in Snow, Ice and Frozen Ground. In: Climate Change 2007: The Physical Science Basis. Contribution of Working Group I to the Fourth Assessment Report of the Intergovernmental Panel on Climate Change [Solomon, S., D. Qin, M. Manning, Z. Chen, M. Marquis, K.B. Averyt, M. Tignor and H.L. Miller (eds.)]. Cambridge University Press, Cambridge, United Kingdom and New York, NY, USA.

Lizotte, M.P., Sharp, T.R., Priscu, J.C., 1996. Phytoplankton dynamics in the stratified water column of Lake Bonney, Antarctica: biomass and productivity during the winter-spring transition. Polar Biology 16:155-162.

Magnuson, J.J., Robertson, D.M., Benson, B.J., Wynne, R.H., Livingstone, D.M., Arai, T., Assel, R.A., Barry, R.G., Card, V., Kuusisto, E., Granin, N.G., Prowse, T.D., Stewart, K.M., Vuglinski, V.S., 2000. Historical Trends in Lake and River Ice Cover in the Northern Hemisphere. Science 289, 1743–1746.

Martens-Habbena, W., Berube, P.M., Urakawa, H., de la Torre, J.R., Stahl, D.A., 2009. Ammonia oxidation kinetics determine niche separation of nitrifying Archaea and Bacteria. Nature 461, 976–979.

Massé, S., Botrel, M., Walsh, D.A., Maranger, R., 2019. Annual nitrification dynamics in a seasonally ice-covered lake. PLoS ONE 14, e0213748.

Mock, T., Gradinger, R., 2000. Changes in photosynthetic carbon allocation in algal assemblages of Arctic sea ice with decreasing nutrient concentrations and irradiance. Marine Ecology Progress Series 202, 1–11.

Morgan-Kiss, R.M., Lizotte, M.P., Kong, W., Priscu, J.C., 2016. Photoadaptation to the polar night by phytoplankton in a permanently ice-covered Antarctic lake. Limnology and Oceanography 61, 3–13.

Newton, R.J., Jones, S.E., Eiler, A., McMahon, K.D., Bertilsson, S., 2011. A Guide to the Natural History of Freshwater Lake Bacteria. Microbiology and Molecular Biology Reviews 75, 14–49.

Özkundakci, D., Gsell, A.S., Hintze, T., Täuscher, H., Adrian, R., 2016. Winter severity determines functional trait composition of phytoplankton in seasonally ice-covered lakes. Global Change Biology 22, 284–298.

Parsons T.R., Maita Y, Lalli, C.M., 1984. A manual of chemical and biological methods for sea water analysis. Deep Sea Research Part A. Oceanographic Research Papers 31, 1523.

Powers, S.M., Baulch, H.M., Hampton, S.E., Labou, S.G., Lottig, N.R., Stanley, E.H., 2017. Nitrification contributes to winter oxygen depletion in seasonally frozen forested lakes. Biogeochemistry 136, 119–129.

Raven, J. A., Kubler, J. E., & Beardall, J. 2000. Put out the light, and then put out the light. Journal of the Marine Biological Association of the United Kingdom, 80(1), 1–25.

Reynolds, Colin S. 2006. Ecology of Phytoplankton. Cambridge University Press, Cambridge.

Rue, G. P., Darling, J. P., Graham, E., Tfaily, M. M., & McKnight, D. M. 2020. Dynamic changes in dissolved organic matter composition in a Mountain Lake under ice

cover and relationships to changes in nutrient cycling and phytoplankton community composition. Aquatic Sciences, 82(1), 15.

Salonen, K., Leppäranta, M., Viljanen, M., Gulati, R.D., 2009. Perspectives in winter limnology: closing the annual cycle of freezing lakes. Aquat Ecol 43, 609–616.

Sharma, S., Blagrave, K., Magnuson, J.J., O'Reilly, C.M., Oliver, S., Batt, R.D., Magee, M.R., Straile, D., Weyhenmeyer, G.A., Winslow, L., Woolway, R.I., 2019. Widespread loss of lake ice around the Northern Hemisphere in a warming world. Nature Climate. Change 9, 227–231.

Sharp, T. R. 1993. Temporal and spatial variation of light, nutrients, and phytoplankton production in Lake Bonney, Antarctica. MSc thesis, Montana State University, pp. 183.

Small, G.E., Bullerjahn, G.S., Sterner, R.W., Beall, B.F.N., Brovold, S., Finlay, J.C., McKay, R.M.L., Mukherjee, M., 2013. Rates and controls of nitrification in a large oligotrophic lake. Limnology and Oceanography 58, 276–286.

Steemann Nielsen, E., 1952. The use of radioactive carbon for measuring organic production in the sea. J. Cons. Int. Explor. Mer. 18, 117–140.

Sterner, R. W., Smutka, T. M., McKay, R. M. L., Xiaoming, Q., Brown, E. T. & Sherrell, R. M. 2004. Phosphorus and trace metal limitation of algae and bacteria in Lake Superior. Limnology Oceanography 49:495–507.

Sterner, R.W., 2008. On the Phosphorus Limitation Paradigm for Lakes. International Review of Hydrobiology 93, 433–445.

Tanabe, Y., Kudoh, S., Imura, S., Fukuchi, M., 2008. Phytoplankton blooms under dim and cold conditions in freshwater lakes of East Antarctica. Polar Biol 31, 199–208.

Tolar, B.B., Ross, M.J., Wallsgrove, N.J., Liu, Q., Aluwihare, L.I., Popp, B.N., Hollibaugh, J.T., 2016. Contribution of ammonia oxidation to chemoautotrophy in Antarctic coastal waters. ISME J 10, 2605–2619.

Twiss, M.R., McKay, R.M.L., Bourbonniere, R.A., Bullerjahn, G.S., Carrick, H.J., Smith, R.E.H., Winter, J.G., D'souza, N.A., Furey, P.C., Lashaway, A.R., Saxton, M.A., Wilhelm, S.W., 2012. Diatoms abound in ice-covered Lake Erie: An investigation of offshore winter limnology in Lake Erie over the period 2007 to 2010. Journal of Great Lakes Research 38, 18–30.

Vick-Majors, T., Priscu, J. Inorganic carbon fixation in ice-covered lakes of the McMurdo Dry Valleys. Antarctic Science, 31, 123-132. (2019).

Vincent, W. F. and Vincent, C. L. 1982. Factors controlling phytoplankton production in Lake Vanda. Can. J. Fish. Aquat. Sci. 39: 1602–1609.

Welschmeyer, N. A. 1994. Fluorometric analysis of chlorophyll a in the presence of chlorophyll b and pheopigments, Limnology and Oceanography, 39.

Wetzel, R., 2001. Limnology: Lake and river ecosystems. Third edition. Academic Press, San Diego.

Wetzel, R., Likens, G. E., 2000. Limnological Analyses. Springer New York.

Weyhenmeyer, G.A., Obertegger, U., Rudebeck, H., Jakobsson, E., Jansen, J., Zdorovennova, G., Bansal, S., Block, B.D., Carey, C.C., Doubek, J.P., Dugan, H., Erina, O., Fedorova, I., Fischer, J.M., Grinberga, L., Grossart, H.-P., Kangur, K., Knoll, L.B., Laas, A., Lepori, F., Meier, J., Palshin, N., Peternell, M., Pulkkanen, M., Rusak, J.A., Sharma, S., Wain, D., Zdorovennov, R., 2022. Towards critical white ice conditions in lakes under global warming. Nature Communications 13.

Winder, M., Schindler, D.E. 2004. Climate change uncouples trophic interactions in an aquatic ecosystem. Ecology, 85, 2100-2106.

Yang, F., Cen, R., Feng, W., Zhu, Q., Leppäranta, M., Yang, Y., Wang, X., Liao, H., 2021. Dynamic simulation of nutrient distribution in lakes during ice cover growth and ablation. Chemosphere 281, 130781.